How do minor mergers promote inside-out growth of ellipticals, transforming the size, density profile and dark matter fraction?

Michael Hilz[1],Thorsten Naab[1]* and J.P. Ostriker[2]

[1] *Max-Planck-Institut für Astrophysik, Karl-Schwarzschild-Str. 1, 85741 Garching, Germany*
[2] *Department of Astrophysical Sciences, Princeton University, Princeton, NJ 08544, USA*

ABSTRACT
There is observational evidence for inside-out growth of giant elliptical galaxies since $z \gtrsim 2 - 3$, which is - in contrast to disk galaxies - not driven by in-situ star formation. Many of the $\sim 10^{11} M_\odot$ systems at high redshift have small sizes $\sim 1 kpc$ and surface brightness profiles with low Sersic indices n. The most likely descendants at $z = 0$ have, on average, grown by a factor of two in mass and a factor of four in size, indicating $r \propto M^\alpha$ with $\alpha \gtrsim 2$. They also have surface brightness profiles with $n \gtrsim 5$. This evolution can be qualitatively explained on the basis of two assumptions: compact ellipticals predominantly grow by collisionless minor (mass-ratio 1:10) or intermediate (mass-ratio 1:5) 'dry' mergers, and they are embedded in massive dark matter halos which support the stripping of merging satellite stars at large radii. We draw these conclusions from idealized collisionless mergers spheroidal galaxies - with and without dark matter - with mass ratios of 1:1, 1:5, and 1:10. The sizes evolve as $r \propto M^\alpha$ with $\alpha < 2$ for mass-ratios of 1:1 (and 1:5 without dark matter halos) and , while doubling the stellar mass, the Sersic index increases from $n \sim 4$ to $n \sim 5$. For minor mergers of galaxies embedded in dark matter halos, the sizes grow significantly faster and the profile shapes change more rapidly. Surprisingly, already mergers with moderate mass-ratios of 1:5, well motivated by recent cosmological simulations, give $\alpha \sim 2.3$ and after only two merger generations (~ 40 per cent added stellar mass) the Sersic index has increased to $n > 8$ ($n \sim 5.5$ without dark matter), reaching a final value of $n = 9.5$ after doubling the stellar mass. This is accompanied by a significant increase of the dark matter fraction (from ~ 40 per cent to $\gtrsim 70$ per cent) within the stellar half-mass radius, driven by the strong size increase probing larger, dark matter dominated regions. For equal-mass mergers the effect is much weaker. We conclude that only a few intermediate mass-ratio mergers ($\sim 3 - 5$ with initial mass-ratios of 1:5) of galaxies embedded in massive dark matter halos can result in the observed concurrent inside-out growth and the rapid evolution in profile shapes. This process might explain the existence of present day giant ellipticals with sizes, $r > 4 kpc$, high Sersic indices, $n > 5$, and a significant amount of dark matter within the half-light radius. Apart from negative stellar metallicity gradients such a 'minor' merger scenario also predicts significantly lower dark matter fractions for $z \sim 2$ compact quiescent galaxies and their rare present day analogues.

Key words: Galaxy

1 INTRODUCTION

Merging is a natural process in hierarchical cosmological models and plays a significant role for the assembly of massive galaxies (e.g. Kauffmann 1996). The most massive objects are elliptical galaxies, which are considered to start forming their stars at a redshift of $z \sim 6$ in a dissipative environment and can rapidly become very massive ($\sim 10^{11} M_\odot$) by $z = 2$ (Kereš et al. 2005; Khochfar & Silk 2006; De Lucia et al. 2006; Kriek et al. 2006; Naab et al. 2007, 2009; Joung et al. 2009; Dekel et al. 2009; Kereš et al. 2009; Oser et al. 2010; Feldmann et al. 2010; Domínguez Sánchez

2011; Feldmann et al. 2011; Oser et al. 2012). Their subsequent evolution is not fully understood yet, as these ellipticals are observed to be already quiescent at $z \sim 2$, on average 4-5 times smaller, and a factor of two less massive than their low redshift descendants (Daddi et al. 2005; Trujillo 2006; Longhetti et al. 2007; Toft et al. 2007; Zirm et al. 2007; Trujillo et al. 2007; Zirm et al. 2007; Buitrago et al. 2008; van Dokkum et al. 2008; Cimatti et al. 2008; Franx et al. 2008; Saracco et al. 2009; Damjanov et al. 2009; Kriek et al. 2009; Bezanson et al. 2009; van Dokkum et al. 2010; Saglia 2010; Whitaker et al. 2012; Onodera 2012). This rapid size evolution eventually proceeds in an inside-out fashion in the absence of significant star formation an is accompanied by an evolution in the light (and eventually mass) distribution (Hopkins et al. 2009; van Dokkum et al. 2010; Auger et al. 2011; Tiret et al. 2011; Szomoru et al. 2012; Saracco et al. 2012). This growth process is distinctively different from the star formation driven inside-out growth of disk galaxies (Prantzos & Aubert 1995; Matteucci & Francois 1989; Mo et al. 1998; Naab & Ostriker 2006; Governato et al. 2007; Wang et al. 2011; Kauffmann et al. 2012). In addition, there is growing observational evidence that high redshift ellipticals are more flattened with exponential like surface brightness distributions ($n \lesssim 4$) whereas their potential present day massive descendants are rounder and have more concentrated profiles shapes with $n \gtrsim 5$ (Toft et al. 2005; Trujillo 2006; Toft et al. 2007; van Dokkum et al. 2008; van der Wel et al. 2008, 2009; van Dokkum et al. 2010; van der Wel et al. 2011; Kormendy et al. 2009; Carrasco et al. 2010; Weinzirl et al. 2011; Buitrago et al. 2011; Kormendy & Bender 2012; Szomoru et al. 2012).

Direct observations of massive compact and quiescent high redshift systems also provide new constraints on the formation histories of giant elliptical galaxies. At face value the dramatic difference in properties of massive quiescent galaxies at high and low redshift rules out a simple 'monolithic' formation followed by simple passive evolution (Kriek et al. 2008; van Dokkum et al. 2008). The observations also rule out the formation of ellipticals in a single 'disk merger' event, a scenario for massive ellipticals which might also suffer from other problems (Ostriker 1980; Naab & Burkert 2003; Burkert et al. 2008; Naab & Ostriker 2009). Even if the progenitor disks were gas-rich leading to a compact remnant (Ricciardelli et al. 2010; Wuyts et al. 2010; Bournaud et al. 2011) those would have to evolve further by a separate process (see e.g. Hopkins et al. 2009).

In addition to the well studied stellar components there is evidence for the existence for dark matter within the half-light radii of ellipticals (Gerhard et al. 2001; Thomas et al. 2009, 2011; Cappellari 2012a). Gravitational lensing measurements of massive galaxies in the local universe predict, on average, ~ 30 per cent of the matter within the half-light radius of present day massive elliptical galaxies being dark matter (Auger et al. 2010; Barnabè et al. 2011). At high redshift, however, the situation is more uncertain (Toft et al. 2012) as dark matter cannot be measured directly. The naive expectation is that dark matter is much less important due to the dissipative nature of the early evolution. Still, assuming its existence and collisionless nature, dark matter will eventually affect the distribution of

stars during the further assembly of the galaxies (see e.g. Lackner & Ostriker 2010; Hilz et al. 2012).

The underlying idealized assumption for the study presented here is that present day massive elliptical galaxies ($> 10^{11} M_\odot$) since $z \sim 2$ have grown predominantly by accreting stars that have formed in other galaxies and this process can be approximated by simulations of mergers of collisionless 'dry' stellar systems. This assumption is not too far fetched as there is clear observational evidence for the predominance of old ($z \gtrsim 2$) stellar populations in these galaxies, leaving little room for gas accretion and subsequent star formation (e.g. Searle et al. 1973; Brinchmann & Ellis 2000; Treu et al. 2005; Thomas et al. 2010; van Dokkum et al. 2010; López-Sanjuan et al. 2010; Young 2011; Crocker 2012). Directly observed mergers, inferred merger rates, as well as stellar fine structure at large galactocentric radii are indicative of stellar merger and accretion events (Malin & Carter 1983; Schweizer & Seitzer 1992; Tran et al. 2005; van Dokkum 2005; Bell et al. 006a,b; Faber 2007; McIntosh et al. 2008; Whitaker & van Dokkum 2008; Robaina et al. 2010; Duc 2011; Lotz et al. 2011; Trujillo et al. 2011; Weinzirl et al. 2011; Tal et al. 2012; López-Sanjuan 2012). On the theoretical side, phenomenological as well as direct numerical studies predict that the late assembly of massive galaxies is dominated by the late accretion of stars that formed early (Kauffmann 1996; De Lucia et al. 2006; Ciotti et al. 2007; Naab et al. 2007; Guo & White 2008; Naab et al. 2009; Yang et al. 2011; Lackner & Ostriker 2010; Oser et al. 2010; Guo et al. 2011; Feldmann et al. 2011; Oser et al. 2012; Yang et al. 2012; Gabor & Davé 2012; Moster et al. 2012; Lackner et al. 2012)). In a previous study Hilz et al. (2012) used idealized merger simulations of spheroidal galaxies to re-investigate the effect of the galaxy merger mass-ratio - limited to the extreme cases of 1:1 and 1:10 - on the merger driven evolution of compact high-redshift spheroids. The main finding of this study was that both minor and major mergers lead to size growth and an increase of the dark matter fraction, however by different physical processes and at significantly different strengths. Violent relaxation in major mergers mixes dark matter into the central regions and escaping particles limit the expected size growth even below the expected values. In 1:10 mergers on the other hand, satellite particles are stripped at large radii where the initial host galaxies are dominated by dark matter. As a result the stellar effective radii and the dark matter fractions of the galaxies grow rapidly.

Here we extend the Hilz et al. (2012) study to focus on the inside-out growth including a moderate mass-ratio of 1:5. This step is important for a number of reasons: The average stellar mass growth since $z \sim 2$ is a factor of two. Mergers with mass-ratios of 1:10 typically take a long time to complete and it is not clear whether ten of these mergers can even be completed in a Hubble time. Additionally, recent observationally estimated merger rates indicate more minor mergers for massive galaxies and at higher redshift but the rates are still low and it is not clear - also theoretically - whether there are enough minor mergers to explain the size growth (Nipoti et al. 009b,a; Williams et al. 2011; Weinzirl et al. 2011; Newman et al. 2012; Nipoti et al. 2012; Cimatti et al. 2012; Man et al. 2012; Edwards & Patton 2012; Mármol-Queraltó et al. 2012). Higher mass-ratio
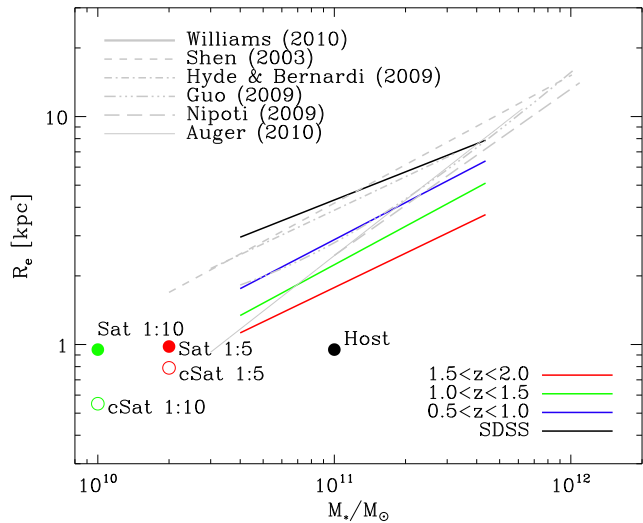
Figure 1. Stellar mass versus effective radius for the initial galaxy models. For our fiducial set of simulations (diffuse satellites) all galaxies have an effective radius of $1kpc$ (filled circles). For the second set of simulations with compact satellites (open circles) the sizes follow the $z = 2$ relation (red line) by Williams et al. (2010). The initial conditions are well separated from local mass-size relations of ellipticals (Shen et al. 2003; Hyde & Bernardi 2009; Guo et al. 2009; Nipoti et al. 009a; Auger et al. 2010).

mergers result in a more rapid mass growth and fewer of them would be needed provided the size grows rapid enough. Another reason to focus on mass-ratios of 1:5 was recently provided by direct cosmological simulations. Three independent numerical studies have found that the average mass-weighted mass ratio of galaxy mergers building massive ellipticals is 1:4 - 1:5, making this regime particularly interesting (Oser et al. 2012; Gabor & Davé 2012; Lackner et al. 2012).

In section 2 we give a short review of the initial galaxy models and the simulation parameters. In the subsequent Sections 3, 4, 5, and 6 we investigate the evolution of sizes, surface densities, profiles shapes and dark matter fractions, respectively. We discuss the results and conclude in Section 7.

2   SIMULATIONS

Continuing the long line of research in this direction (White 1978, 1979; Miller & Smith 1980; Villumsen 1983; Farouki et al. 1983; Nipoti et al. 2003; Boylan-Kolchin et al. 2005; Ciotti et al. 2007; Nipoti et al. 009b) we present a set of simulations of dissipationless mergers of spheroidal galaxies with and without dark matter halos and with mass ratios of 1:1, 1:5, and 10:1. Details about the initial models and the simulations parameters for 1:1 and 1:10 mergers are presented in Hilz et al. (2012). The simulations were performed with the N-body/SPH code $VINE$ (Wetzstein et al. 2009; Nelson et al. 2009). For the present study we have also performed comparison

run with $GADGET$ (Springel 2005) with identical results. Here we only give a brief summary of the simulation setup. The initial galaxy models are isotropic, spherically symmetric one- and two-component systems following Hernquist density profiles (Hernquist 1990) either for a model representing only the stellar component of the galaxy (one-component, bulge-only) or a bulge embedded in a massive dark matter halo (two-component, bulge+halo). The host bulges have a stellar mass of $M_{*,\mathrm{host}} = 1$ and a scale radius of $a_{*,\mathrm{host}} = 1.0$ (corresponding to a projected half-mass radius of $R_\mathrm{e} \sim 1.8a_{*,\mathrm{host}}$ (Hernquist 1990) realized with 100.000 particles. For the two-component cases we assume an additional dark matter halo with a total dark to stellar mass ratio of $M_{\mathrm{dm}}/M_* = 10$ and a ratio of the scale radii of $a_{\mathrm{dm}}/a_* = 11$. The halo is realized with 1.000.000 particles resulting in equal-mass particles for both components. The gravitational softening length is set to $\epsilon = 0.02$ for all particles. The stability of the initial N-body models was demonstrated in Hilz et al. (2012). The merging satellite galaxies are 5 (mass-ratio 1:5) or 10 times (mass-ratio 1:10) less massive than the host and have a correspondingly lower particle number. For our fiducial set of simulations we assume the same scale radius, $a_{*,\mathrm{sat}} = 1.0$, for all bulges, resulting in satellites being more diffuse than the host. For a second set of simulations we chose more compact satellites with scale radii of $a_{*,\mathrm{sat}} = 0.8$ for the 1:5 mergers and $a_{*,\mathrm{sat}} = 0.5$ for the 1:10 mergers following a $z \sim 2$ mass-size relation (Williams et al. 2010).

The open and filled circles in Fig. 1 indicate the location of the initial galaxy models in the mass-size plane compared to several published present day and high redshift mass-size relations. The initial massive host galaxies resemble typical massive and compact 'red nuggets' at $z = 2$ which are smaller than typical present day galaxies at $10^{11} M_\odot$ (red line from Williams et al. 2010). However, for redshift two galaxies below $\sim 4.0 \times 10^{10} M_\odot$ (which would be the minor merger partners) there is no consistent size information available. Therefore we assume two scenarios: a fixed size of $\sim 1kpc$ for the satellites, similar to local galaxies (see e.g. Misgeld & Hilker 2011), indicated by the filled red and green circles. Here the merging lower mass galaxies are diffuse spheroids with low phase space densities comparable to low mass disk-like galaxies. Alternatively we use smaller sizes consistent with a simple continuation of the $z = 2$ mass-size relation to lower masses (open circles), resulting in compact spheroids.

The first generation of equal-mass mergers are parabolic mergers of one- and two-component models of the initial host galaxies. The second generation is a re-merger of the duplicated, randomly oriented, first generation merger remnant, which was allowed to dynamically relax at the center. The randomly oriented galaxies approach each other on parabolic orbits with a pericenter distance of half the spherical half-mass radius of the progenitor remnants, i.e. the pericenter distances increase with each merger generation. The sequences of intermediate and minor mergers with initial mass-ratios of 1:5 (1:10) are also simulated with one- and two-component models. In the following we use the traditional convention to call all mergers with mass-ratios smaller than 1:4 minor mergers. Initially, the mass-ratio is 1:5 (1:10) and the galaxies are set on parabolic orbits. The randomly oriented merger remnants of the first generations are then
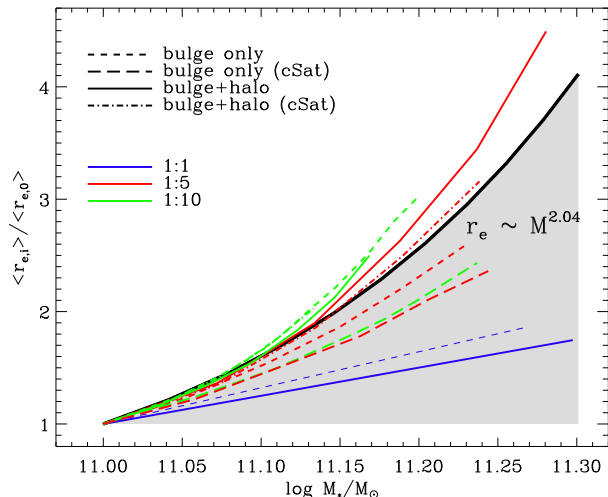
Figure 2. The projected spherical half-mass radius of the stellar component (the mean value along the three principal axes) as a function of bound stellar mass for 1:1 (blue), 1:5 (red), and 1:10 (green) mergers. The observed size growth is indicated by the solid black line (see van Dokkum et al. (2010) for the observational uncertainties). The size evolution of models in the grey shaded area is too weak to be consistent with observations. All mergers of bulges embedded in massive dark matter halos and high mass-ratios (1:5, 1:10, red and green solid/dashed-dotted lines) show a rapid size evolution. The size evolution of the bulge-only models (short and long dashed lines) are not efficient enough, except the 1:10 scenario with a diffuse satellite (green dashed line). The accretion of compact satellites results in less size growth compared to the diffuse satellites. The major merger lines (blue) show size growth that is far too slow.

set on parabolic orbits with the initial satellite galaxy models and a mass-ratio of now 1:6 (1:11), and so on. We perform 6 generations of 1:10 mergers and 5 generations of 1:5 mergers using satellites with fixed scale radii (Sat 1:5/1:10, see Fig. 1). For comparison, we also performed minor mergers of two-component models with compact satellites (cSat 1:5/1:10, see Fig. 1). Again all parabolic orbits have pericenter distances of half the spherical half-mass radius of the bulge of the massive progenitor galaxy.

The 1:10 bulge-only simulations have no dark matter halo and the in-falling satellites suffer less from dynamical friction. Therefore the final coalescence takes by far the longest time. However, taking about ~ 9 Gyrs for 10 merger generations even this process could be completed by the present day assuming a $z = 2$ progenitor. All other merger series are completed in less than ~ 7 Gyrs.

3 EVOLUTION OF THE SIZES

After the completion of every merger, we allow the central region of the remnant to relax, before we compute the projected circular half-mass radii, r_e, along the three principal axes and the bound stellar (bulge) mass, M_*.

In Fig. 2 we show the evolution of the half-mass radius as a function of the bound stellar mass for 1:1 (blue), 1:5 (red), and 1:10 (green) merger hierarchies. The black line indicates the observed evolution, $r_e \propto M^{2.04}$, in the mass-

size plane from $z \sim 2$ to the present day (van Dokkum et al. 2010). The models here are idealized in the sense that they do not contain any dissipative component. If present, like in the 'real' universe, this component would reduce the size growth per added mass (Dekel & Cox 2006). Therefore we consider a model a failure if it occupies the the shaded area in Fig. 1. Promising models have to lie above this line so that small amounts of gas - and therefore somewhat smaller sizes - can be tolerated.

Equal-mass mergers show an almost linear increase of size with mass, (see also Boylan-Kolchin et al. 2005; Ciotti et al. 2007; Bezanson et al. 2009; Nipoti et al. 009b; Hilz et al. 2012), independent of whether the stellar system is embedded in a dark matter halo or not (blue solid and dashed lines). As discussed by Boylan-Kolchin et al. (2005), in mergers with dark matter halos the in-falling galaxy suffers more from dynamical friction in the massive dark matter halo of the companion galaxy, resulting in more energy transfer from the bulge to the halo, leading to a more tightly bound bulge with a smaller size (blue solid line, Fig. 2) compared to the model without dark matter (blue dashed line, Fig. 2). If we combine the results of both major merger scenarios this yields a mass-size relation of $r_e \propto M^{0.91}$ which is comparable to the results of Boylan-Kolchin et al. (2005), who found a slightly smaller exponent (~ 0.7) for orbits with high angular momentum and an exponent ~ 1 for pure radial orbits. Nevertheless, as the size grows at most linearly with mass, dissipationless major mergers cannot be the main driver for the size evolution of early-type galaxies.

As expected from simple virial estimates (Cole et al. 2000; Ciotti et al. 2007; Naab et al. 2009; Bezanson et al. 2009), the size evolution is stronger for bulge-only models with lower mass-ratios of 1:5 and 1:10 (red and green lines in Fig. 2). However, except for the 1:10 mergers with a diffuse satellite (green short dashed line), all minor mergers with bulge-only satellites are not efficient enough to escape the 'forbidden' area. This behaviour is improved for minor mergers of two-component models, where bulges are embedded in a massive dark matter halos. For mass-ratios 1:5 and 1:10 the size evolution is in excess of the observed evolution. In the case of 1:5 minor mergers with a less compact satellite (red solid line), we obtain a mass-size growth relation of $r_e \propto M^{2.4}$ with a similar or even larger exponent for both two-component 1:10 scenarios. Therefore we consider all minor merger models (1:5 and 1:10) with dark matter halos and the diffuse 1:10 mergers to be consistent with observations even in more realistic models, where dissipational effects would reduce the size growth (Robertson et al. 2006; Cox et al. 2006; Hopkins et al. 2008; Covington et al. 2011). The size growth via major mergers is too slow to fit observational data.

4 EVOLUTION OF THE SURFACE DENSITIES

We now take a closer look at the evolution of the surface densities of the merger remnants. In Fig. 3, we plot the stellar surface mass densities and cumulative stellar mass profiles after every 1:1 and 1:5 merger and every second 1:10 merger for bulge-only models (top panels) and bulge+halo models (bottom panels). For equal-mass mergers there is mass growth at all radii, i.e. the lines are shifted more or
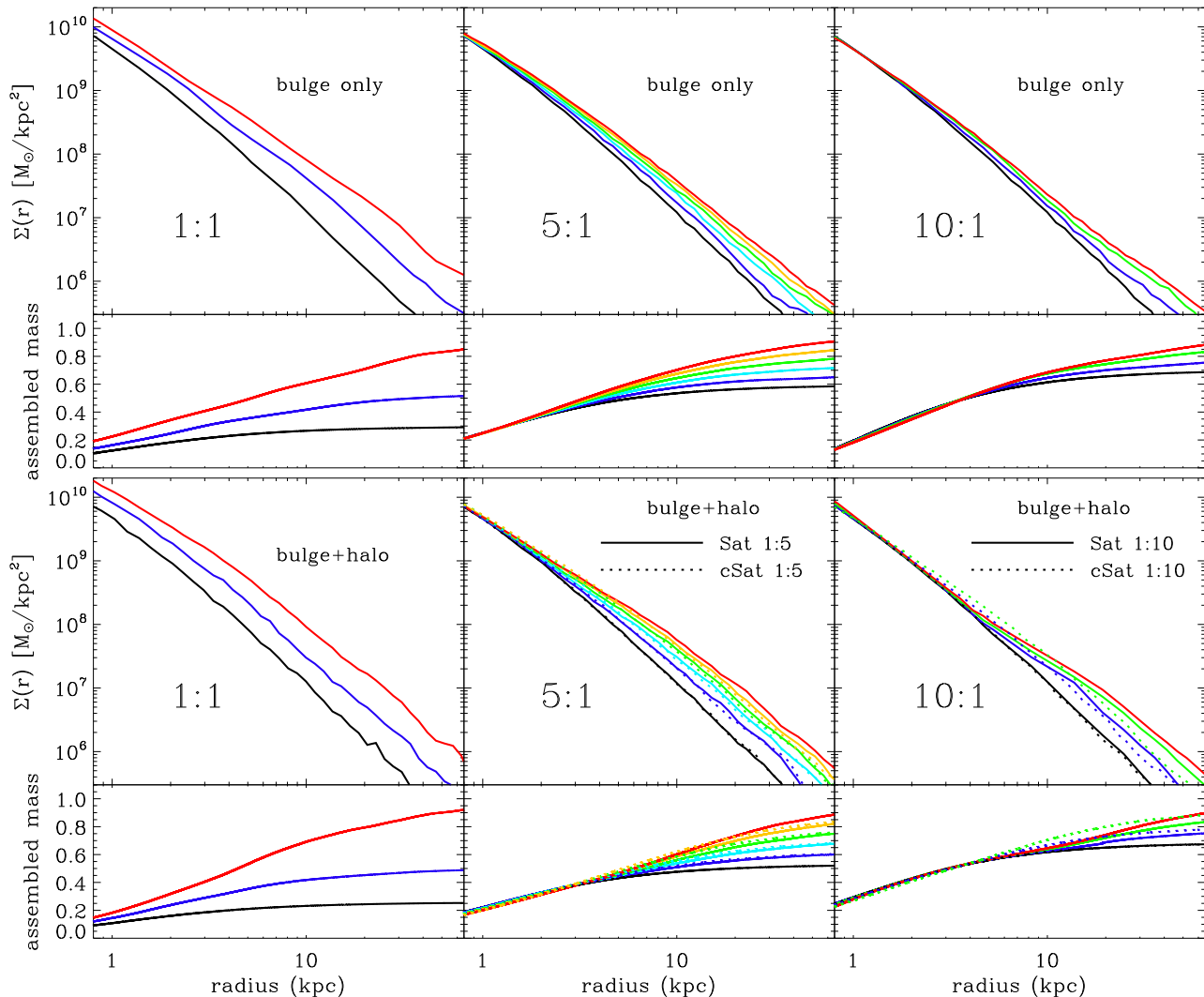
Figure 3. Top panels: Stellar surface mass density profiles and cumulative stellar mass distributions for the fiducial 1:1 (left), 1:5 (middle) and 1:10 (right) bulge-only merger models after each merger event (colored lines from bottom to top, for 1:1 and 1:5 mergers we show every generation, for 1:10 mergers every second). For all mass-ratios the surface densities increase at all radii with merger generation with a trend of a stronger increase in the outer regions for lower mass-ratios. Bottom panels: Same for mergers of systems with dark matter halos. Equal-mass mergers show a similar behaviour than bulge-only models. For 1:5 and 1:10 bulge+halo models (mergers with compact satellites are indicated by the dotted lines) the inside-out growth trend is stronger than for bulge-only models. Regions inside 4kpc are almost unaffected and the satellite stellar mass assembles predominantly at large radii similar to observations van Dokkum et al. (2010).

less parallel to higher densities independent of the presence of a halo (see e.g. Miller & Smith 1980; Villumsen 1983; Farouki et al. 1983 for discussions on the weak but existing break of homology). This evolution scenario would be in disagreement to observations of van Dokkum et al. (2010), which show, that early-type galaxies grow inside-out, i.e. the central densities stay constant and most of the mass assembles at larger radii, building up an extended envelope of stars.

The second column in Fig. 3 depicts the surface densities and mass assembly of minor mergers with an initial mass ratio of 1:5. For the bulge-only models (top) with a diffuse satellite (Sat 1:5, Fig. 2), the surface density stays nearly constant up to $r \sim 1 - 2$kpc and increases mainly in the

outer parts. This effect was already reported by Villumsen (1983) as a possible explanation for abundance gradients in elliptical galaxies. The same scenario leads to an even stronger inside-out growth if the galaxies are surrounded by a dark matter halo (bottom panel, second column). Here the bulge particles get stripped at larger radii and the central surface density ($r < 4$kpc) stays unaffected; it only increases at radii $r > 2 - 3$kpc. The size growth shown in Fig. 2 is due to this build-up of a massive stellar envelope. The mass is added to large radii where, prior to the merger, the dark matter component was large. Due to our accounting procedure the dark matter fraction within r_e increases, even though the dark matter added in such mergers to the inner parts is negligible. The dotted lines in these panels show
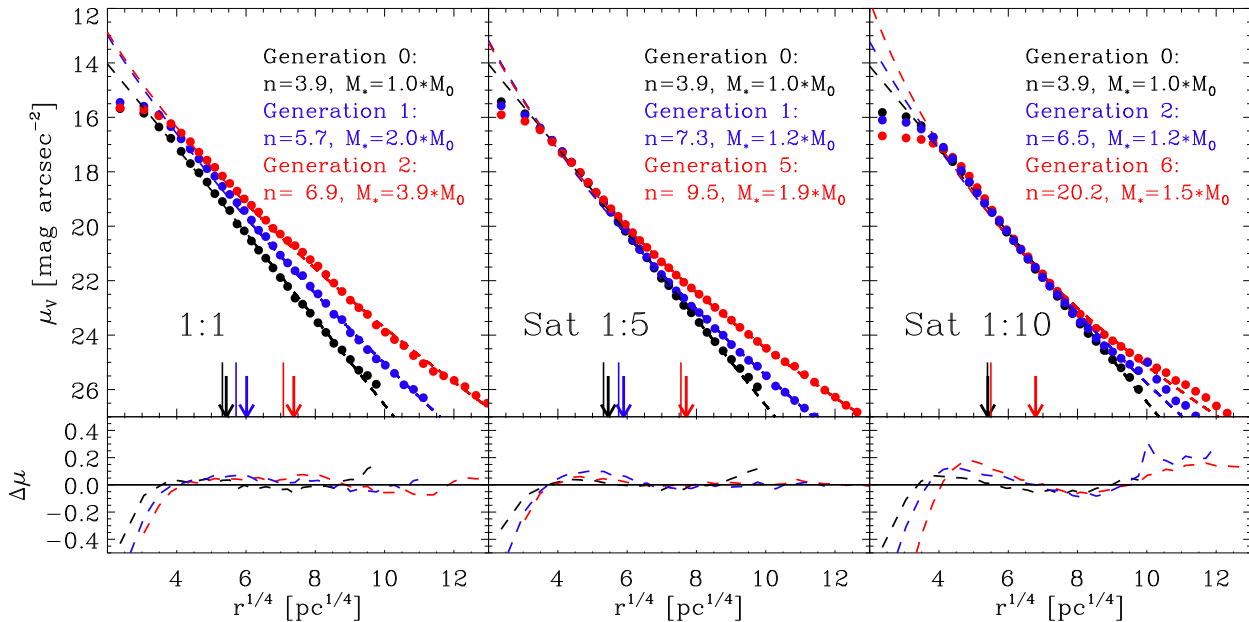
Figure 4. Surface brightness profiles $\mu_V(r)$ of the fiducial two-component 1:1 (left), 1:5 (middle), and 1:10 (right) merger remnants as a function of radius for the initial conditions (black circles), the first merger generation (blue circles, for 1:10 we show the second generation) and the final remnants (red circles). The over-plotted dashed lines show the best fitting Sersic function for the outer profiles. The data was fitted from $0.02r_e$ to either $10r_e$ or a limiting surface brightness of $m_V = 27\text{mag/arcsec}^2$. The residuals $\Delta\mu < 0.2\text{mag/arcsec}^2$ (lower panels) are small, except for the 1:10 case, which cannot be reasonably well fitted anymore for late generations ($n > 20$) The fitted effective radii $r_{e,\text{fit}}$ (short vertical lines) are slightly smaller than the projected half-mass radii r_e (arrows). For minor mergers - 1:5 and 1:10 - the best fitting Sersic index n increases rapidly as the mass added in minor mergers grows. Note that for minor mergers the central surface densities decline the most even as the outer surface densities (and Sersic indices) increase.

the four remnants, where the satellites are more compact (cSat 1:5, Fig. 2) and lie an extension of the $z \sim 2$ mass-size relation. Obviously, the results are very similar.

The six generations of minor mergers with an initial mass-ratio of 1:10 are shown in the right column of Fig. 3. In the case of bulge-only models (top panels), the surface density increases predominantly at larger radii, similar to the previous scenario, but now the satellite stars are even less bound compared to the 1:5 case and therefore are stripped at larger radii, even without a dark matter halo. If present, this effect is enhanced (lower panels of right column), as the satellites first orbit through the massive dark matter halo - and lose stars - before they reach the center of the host. The surface densities are unaffected inside $r = 5$kpc. In summary, 1:5 and 1:10 mergers lead to a significant change in the mass distribution of the galaxies with most of the stellar satellite material assembling at large radii. This picture hardly changes for compact satellites (cSat, dotted lines), although the scale lengths of the satellite stars are significantly smaller, they are more bound and resists the drag force of the host potential for a longer time. Consequently, somewhat more material gets closer to the central regions. In summary a minor merger driven evolution scenario - in particular for 1:5 bulge+halo mergers - is in good agreement with the picture we get from observations. Although we are definitely affected by poor numerical resolution at the very centers of the galaxies we note the differential effect that for minor mergers the central surface densities decline the

most even as the outer surface densities (and Sersic indices) increase in agreement with expectations from recent observations (Szomoru et al. 2012; Trujillo et al. 2012).

5   EVOLUTION OF PROFILE SHAPES

The curvature of the light profiles of elliptical galaxies is an important parameter as it correlates with other observed properties of elliptical galaxies, such as the effective radius r_e, the total luminosity and the stellar mass (Caon et al. 1993; Nipoti et al. 2003; Naab & Trujillo 2006; Kormendy et al. 2009). We therefore use a Sersic $r^{1/n}$ (Sersic 1968) function to fit synthetic surface brightness profiles of our simulations,

$$I(r) = I_e \cdot 10^{-b_n((r/r_e)^{1/n}-1)}, \tag{1}$$

where the three free parameters are the effective surface brightness I_e, the effective radius r_e and the so called Sersic index n. Here, $n = 1$ corresponds to an exponential profile and $n = 4$ to the familiar de Vaucouleurs profile (de Vaucouleurs 1948). The factor b_n, is chosen such that the effective radius r_e encloses half of the total luminosity. For the expected range of Sersic indices, this factor can be approximated by the relation $b_n = 0.868n - 0.142$ (Caon et al. 1993). We convert the projected surface mass densities discussed in section 3 to a V-band surface brightness profile assuming a stellar age of 10^{10}yr and solar metallicity $Z = 0.02$

(Bruzual & Charlot 2003) which is then fitted with a Sersic function (see Naab & Trujillo (2006) for details of the fitting procedure). Those population properties are reasonable for present day massive ellipticals (Thomas et al. 2010) but not necessarily so for higher redshifts. However, details of the choice of population age and abundance are unimportant for the determination of the profile shape (which are the same as for the surface density profiles) as long as we assume a constant mass-to-light ratio (for the stellar component) with radius.

Figure 4 shows examples of the Sersic fits to the surface brightness profiles and the residuals of our fiducial bulge+halo mergers with mass-ratios of 1:1 (left), 1:5 (middle) and 1:10 (right). The profiles are fitted from $0.02r_e$ to either $10r_e$ or to a limiting surface brightness of $m_V = 27$ mag/arcsec^{-2} (Trujillo et al. 2004; Kormendy et al. 2009). The residuals are very small ($\Delta\mu < 0.2$mag/arcsec^2), except for the innermost regions, where the profiles are affected by insufficient sampling, softening and relaxation effects. The initial Hernquist spheres (black circles in all panels) have a Sersic index of $n = 3.9$ (see also Naab & Trujillo 2006). In all cases the fitted Sersic profiles overestimate the central surface brightness leading to a slightly smaller fitted effective radius $r_{e,\mathrm{fit}}$ (narrow vertical lines at the bottom of each surface brightness panel) than the projected half-mass radius r_e (corresponding arrows) presented in Fig. 2. The differences are small and do not affect any conclusions in the paper.

In the case of 1:1 mergers of two-component models (left panel, Fig 4), we can see that the profile shape hardly changes for the remnants. The Sersic index increases weakly from $n = 3.9$ to $n = 5.5$ with a corresponding increase of mass by a factor of about two, hardly enough to explain the very high numbers observers find for large massive elliptical galaxies ($n \sim 10$, see Caon et al. 1993; Kormendy et al. 2009). This picture changes dramatically for minor mergers where the Sersic index increases rapidly to values of $n \sim 10$ for a similar increase in mass. This is a direct consequence of the different evolution of the surface density profiles discussed in section 4.

In Fig. 5 we show, for all fiducial bulge-only and bulge+halo models, the evolution of the Sersic index as a function of the assembled bound stellar mass. There is only a moderate increase in Sersic index for the equal-mass mergers. In contrast, after two generations of 1:5 mergers with a mass increase of of only 40 per cent the Sersic index can be $n > 7$ (for the bulge+halo model) and the final remnant reaches values of $n \sim 9.5$, which is in the range of the observed present day massive elliptical galaxies (Caon et al. 1993; Kormendy et al. 2009). The corresponding bulge-only minor merger scenarios (red and green dashed lines in Fig. 5) show similar but weaker trends yielding final Sersic indices of $n \sim 7.5$. Still, the overall evolution is much faster for two-component models. This again indicates that the merger mass-ratio and dark matter halos play an important role as they increase the effect of stripping at large radii in a way, that the accreted stellar mass assembles at the 'right' regions of the host galaxy.
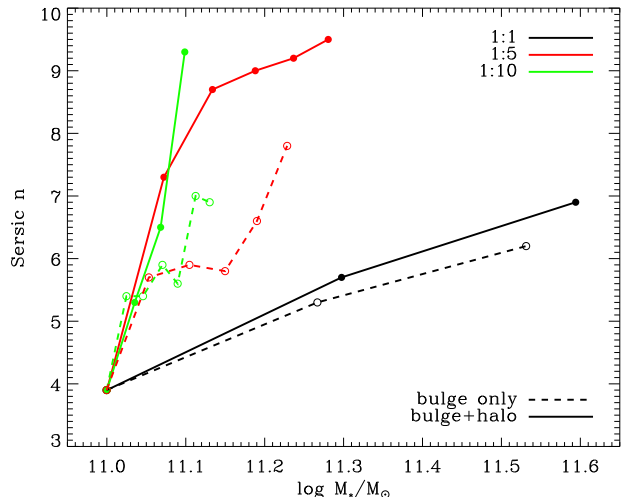

Figure 5. Evolution of the Sersic indices for all fiducial major and minor merger remnants shown in Fig. 4 as a function of bound stellar mass (the evolution for compact satellites is similar). All equal-mass mergers show a very weak evolution (black lines). Lower mass-ratios lead to a stronger evolution for 1:5 (red dashed) and 1:10 (green dashed) bulge-only models. The presence of a dark matter halos even enhances this effect as more stars are deposited at large radii (red and green solid lines). The 1:5 two-component model shows the strongest evolution reaching values of $n > 9$ after mass increase of only 50 per cent. For 1:10 mergers we only show the first generations with reasonable Sersic fits. Later generations cannot be accurately fitted anymore (see Fig. 4).

6 EVOLUTION OF DARK MATTER FRACTIONS

In this section we investigate the dark matter fractions within the effective radii of our simulated merger remnants in the light of recent lensing observations, which predict an increasing dark matter fraction for more massive ellipticals (Auger et al. 2010; Barnabè et al. 2011), dynamical modeling (Gerhard et al. 2001; Cappellari 2012a) and the possibly low dark matter fractions in high redshift galaxies (Toft et al. 2012). The dark matter fractions f_{dm} for all bulge+halo simulations

$$f_{dm}(r < r_{50}) = M_{dm}(r < r_{50})/M_{tot}(r < r_{50}) \qquad (2)$$

are shown in Fig. 6 as a function of assembled stellar mass. Here r_{50} denotes the spherical half-mass radius of the stellar component and M_{dm}, M_{tot} are the halo mass and total mass within r_{50}. We have already explained how the observable f_{dm} will increase simply by accounting, when the stars are added far out in the dark matter halo. The dark matter fraction increases rapidly with each subsequent minor merger generation regardless of the mass-ratio. For a mass increase of a factor of two the dark matter fractions increases by almost a factor two from ~ 40 per cent to $\gtrsim 70$ per cent for minor mergers whereas equal-mass mergers only an increase to ~ 55 per cent. The strong evolution with added mass for minor mergers is a consequence of the rapid size growth (Fig. 2), which is in good agreement with (Nipoti et al. 009b). The evolution of f_{dm} correlates with the radii of the merger remnants. Therefore the 1:5 scenario
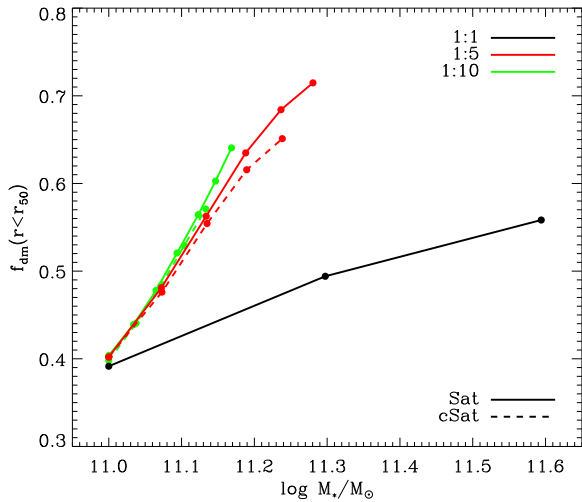
Figure 6. Evolution of the dark matter fraction, $f_{dm}(r < r_{50}) = M_{dm}(r < r_{50})/M_{tot}(r < r_{50})$, within the spherical half-mass radius r_{50} (which is similar to the half mass radius) for all bulge+halo models as a function of bound stellar mass of the merger remnants. Equal-mass mergers show a weak increase of f_{dm}. A very rapid increase of f_{dm} is found for 1:5 (red) and 1:10 (green) mergers, with a similar evolution for compact satellites (dashed lines). The evolution of f_{dm} for 1:5 mergers with mass is very similar to 1:10 mergers indicating that less events results in similar change of f_{dm}.

with more compact satellites (red dashed line), which shows slightly weaker size growth than the fiducial case (Fig. 2), also has a slightly lower dark matter fraction. On the other hand, the 1:10 bulge+halo remnants grow rapidly in size and therefore have the highest dark matter fractions. It is easy to understand this trend. As noted, the dark matter is not pushed inwards; rather we are adding stars to the outer, dark matter dominated parts of galaxies so naturally the amount of dark matter within the stars increases. A detailed analysis of this process can be found in Hilz et al. (2012).

7   DISCUSSION AND CONCLUSION

We present idealized binary merger simulations of spheroidal galaxies with initial mass-ratios of 1:1, 1:5, and 1:10 represented by pure bulges and bulges embedded in dark matter halos. The 1:5 mass-ratio is of particular interest as it is similar to the average mass weighted galaxy merger mass-ratio driving the assembly of massive galaxies recently published cosmological simulations and therefore those minor mergers (or intermediate mass-ratio mergers, traditionally all mergers with mass ratios smaller than 1:4 are called minor mergers) represent a typical growth mode (Oser et al. 2012; Gabor & Davé 2012; Lackner et al. 2012). With this study we aim at assessing the effect of pure collisionless major and minor mergers on the structural evolution for an already existent, observed, high-redshift population of compact and massive galaxies (see e.g. Bournaud et al. (2007) for a discussion on the effect of repeated minor mergers on disks).

Confirming earlier studies we find that major merg-

ers alone cannot explain the observed size growth but minor mergers with mass-ratios of 1:5 or 1:10 show a significantly stronger size growth per added stellar mass (Khochfar & Silk 2006; Naab et al. 2009; Nipoti et al. 009a; Hopkins et al. 2010; Hilz et al. 2012; Oser et al. 2012). This effect is slightly enhanced for more diffuse satellites and significantly enhanced if the galaxies are surrounded by dark matter halos. In these cases the satellite stars are more efficiently stripped at larger radii, either because they are less bound or because they orbit in the deeper potential wells of the dark matter halos. The latter effect (see Hilz et al. (2012) for a detailed discussion) leads to an inside-out size growth of $r \propto M^{2.3}$ already for mergers with a mass-ratio of 1:5, in agreement with observations (van Dokkum et al. 2010; Szomoru et al. 2012). Overall, the picture is very similar to the dynamical friction driven galactic cannibalism described by Hausman & Ostriker (1978) as an explanation for BCG properties (Ruszkowski & Springel 2009; Laporte et al. 2012).

The inside-out assembly of mass at larger radii results in a significant change of the surface density profiles which is here quantified by an increase of the Sersic index n. Starting at a fiducial value of $n = 4$ the increase is weak for major mergers but very strong for minor mergers of galaxies embedded in dark matter halos. In the most extreme case only two 1:5 mergers of bulges with dark matter halos change the Sersic index from $n \sim 4$ to $n \sim 8.5$ at a concurrent stellar mass increase of only 40 per cent. We note that $n = 4$ is the fiducial starting point of the specific simulation setup we have chosen. Qualitatively a similar increase in Sersic index is expected for smaller, and probably more realistic, starting values of $n \sim 2$ for quiescent high redshift galaxies. In this case the maximum Sersic index might not reach as high values as presented here but more accurate predictions are beyond the scope of idealized collisionless studies like the one presented here. Major merger scenarios with disk-like progenitors do also result in an increase of the Sersic index but accompanied by a very weak size increase or even a reduction in size in the presence of gas (Naab & Trujillo 2006; Robertson et al. 2006; Cox et al. 2006; Hopkins et al. 2008; Wuyts et al. 2010). Here the increase in Sersic index is partly driven by dissipative processes at the center of the remnants. Consistent with the results presented here, even considering subsequent 'dry' major mergers keep the Sersic indices for the main stellar body low at $n \lesssim 5$. (Naab & Trujillo 2006; Hopkins et al. 2009). Therefore a minor merger driven scenario - the late addition of old stars at large radii - provides a powerful explanation for the predominance of high Sersic indices of present day large and massive ellipticals (Graham et al. 2001; Trujillo et al. 2004; Kormendy et al. 2009; Hoyos 2011; Kormendy & Bender 2012) some of which are most likely the descendants of compact 'red and dead' flattened high-redshift galaxies with lower Sersic indices (van Dokkum et al. 2008; van der Wel et al. 2009; Bundy et al. 2010; Wuyts et al. 2010; Buitrago et al. 2011; Wuyts 2011; van der Wel et al. 2011; Szomoru et al. 2012).

Naturally, major mergers are also expected to happen during the assembly of massive galaxies. There is direct and indirect observational evidence for this but the expected rates are low ($\sim 0.5 - 2$ since $z \sim 2$) (Bell et al. 006a; McIntosh et al. 2008; van der Wel et al. 2009; Robaina et al. 2010; Williams et al. 2011; Newman et al.

2012; Man et al. 2012; López-Sanjuan 2012). A major merger will definitely dominate the late mass assembly history of the galaxy with a significant impact on its abundance gradients, kinematics and, eventually, morphology (White 1978; Naab et al. 2006; Bois 2011). However, as we have shown here, the expected evolution in size, surface density profile shapes and, eventually, dark matter fraction will be only moderate and not sufficient to evolve the compact high-redshift population into present day ellipticals. Another argument against major mergers driving the size evolution is the apparent absence (or very low number) of massive compact galaxies in the present day universe (Trujillo et al. 2009; Taylor et al. 2010). Due to the low rates a significant number of massive galaxies will not have experienced any major merger since $z \sim 2$ and would remain compact (Bezanson et al. 2009). Nevertheless, a few massive compact have been found which eventually are relics of the high redshift population or have formed recently in a similar manner (Valentinuzzi et al. 2010; Jiang et al. 2012; Trujillo et al. 2012; Ferré-Mateu et al. 2012). Consistent with our framework these galaxies have low Sersic indices and our model predicts lower dark matter fractions compared to normal sized present day giant elliptical galaxies of similar mass.

The evolution of dark matter fractions within the observable stellar half-mass radius is also significantly different for major and minor mergers. In the equal-mass mergers presented here the dark matter fraction increases from the fiducial starting value of ~ 40 per cent to ~ 48 per cent for a stellar mass increase of a factor of two. This increase is driven by mixing processes during the violent merger process which lead to a real change in the radial distribution of luminous and dark matter (Hilz et al. 2012, see also Boylan-Kolchin et al. 2005). For the same increase in mass, minor mergers (e.g. 1:5) result in a four times stronger increase of the dark matter fraction (from ~ 40 per cent to $\gtrsim 70$ per cent). Here the host galaxy structure is only weakly affected but the effective radius of the stellar distribution increases significantly into regions which were ab-inito dominated by dark matter. Therefore only the ruler with which the galaxies are measured is changing (Hopkins et al. 2009; Cenarro & Trujillo 2009; Lackner & Ostriker 2010; Hilz et al. 2012). We note that the exact numbers for the final dark matter fractions are determined by our choice of the initial dark matter fraction. Our fiducial starting value of ~ 40 per cent might in reality be lower for massive high-redshift galaxies but also in this case we expect similar trends. There is evidence for the presence of dark matter in present day massive ellipticals, however the exact amount is uncertain (Gerhard et al. 2001; Thomas et al. 2009, 2011; Cappellari 2012a). Most recent lensing observations indicate dark matter fractions (with large uncertainties) in the range of 20-50 per cent with higher fractions for more massive galaxies (Auger et al. 2010; Barnabè et al. 2011). These trends are easy to reconcile in the context of an evolutionary scenario where the early formation of ellipticals is dominated by a dissipative formation with little dark matter at the center (see (Toft et al. 2012) for tentative observational evidence) followed by a dissipationless assembly dominated by minor mergers naturally increasing the dark matter fractions. This increase would be larger for more massive galaxies which assemble more mass by late stellar merg-

ers (see e.g. De Lucia et al. 2006; De Lucia & Blaizot 2007; Guo & White 2008; Oser et al. 2010, 2012; Lackner et al. 2012). However, predicted dark matter fractions depend sensitively on assumptions about the stellar initial mass function and recent evidence for rising stellar mass-to-light ratios with stellar mass leave less room for the presence of dark matter (van Dokkum & Conroy 2010; Cappellari 2012b; Conroy & van Dokkum 2012; van Dokkum & Conroy 2012; Ferreras et al. 2012).

More quantitative predictions, some based on simple binary merger simulations of spheroids similar to the ones presented here, in a cosmological context have been attempted and come to varying conclusions; some agree with observations (Ciotti et al. 2007), some highlight possible tension with observational trends (Nipoti et al. 009b,a; Cimatti et al. 2012; Nipoti et al. 2012; Quilis & Trujillo 2012). However, the quantitative predictive power of such studies is limited by construction as a realistic cosmological assembly of massive galaxies is very complex and many details depend on the model assumptions about the structure of the galaxies and the satellites, galaxy orbits, gas fractions, merger rates etc. Qualitatively, however, our results are in good agreement with high-resolution cosmological simulations (Feldmann et al. 2010; Oser et al. 2012; Lackner et al. 2012), which are supposedly the method of choice to evaluate these processes in more detail in the future.

The predictions of this simple - dark matter assisted - minor merger driven evolution model are in good qualitative agreement with careful observations of the structural redshift evolution of early-type galaxies (van Dokkum et al. 2010; Weinzirl et al. 2011; Buitrago et al. 2011; Szomoru et al. 2012; McLure et al. 2012). We note here that we have tested for the extreme case of compact progenitors. A significant fraction of high redshift ellipticals have larger sizes (Mancini et al. 2010; Szomoru et al. 2012) and would require relatively little evolution and less mergers. All the above effects are expected to be stronger for more massive galaxies which are expected to have a larger fraction of their stars acquired in accretion events. The most extreme cases would be centrals in galaxy clusters (Ostriker & Hausman 1977; Dubinski 1998; De Lucia & Blaizot 2007; Ruszkowski & Springel 2009; Laporte et al. 2012).

If we are right, then certain definite and testable predictions can be made about the properties of the outer parts ($r > r_e$) of normal giant ellipticals: Since they are the result of accretion of low mass systems they should have considerably lower metallicities than the inner parts. Steeper gradients at large radii then might imply a formation history dominated by minor mergers (White 1978; Kobayashi 2004, see however Pipino et al. 2010 for an alternative view). The stellar orbits at large radii should become radially biased (Hilz et al. 2012) and the dark matter fractions of massive ellipticals should increase rapidly at large radii.

ACKNOWLEDGMENTS

REFERENCES

Auger M. W., Treu T., Bolton A. S., Gavazzi R., Koopmans L. V. E., Marshall P. J., Moustakas L. A., Burles S., 2010, ApJ, 724, 511

Auger M. W., Treu T., Brewer B. J., Marshall P. J., 2011, MNRAS, 411, L6

Barnabè M., Czoske O., Koopmans L. V. E., Treu T., Bolton A. S., 2011, MNRAS, 415, 2215

Bell E. F., Naab T., McIntosh D. H., Somerville R. S., Caldwell J. A. R., Barden M., Wolf C., Rix H.-W., Beckwith S. V., Borch A., Häussler B., Heymans C., Jahnke K., Jogee S., Koposov S., Meisenheimer K., Peng C. Y., Sanchez S. F., Wisotzki L., 2006a, ApJ, 640, 241

Bell E. F., Phleps S., Somerville R. S., Wolf C., Borch A., Meisenheimer K., 2006b, ApJ, 652, 270

Bezanson R., van Dokkum P. G., Tal T., Marchesini D., Kriek M., Franx M., Coppi P., 2009, ApJ, 697, 1290

Bois M. e. a., 2011, MNRAS, 416, 1654

Bournaud F., Chapon D., Teyssier R., Powell L. C., Elmegreen B. G., Elmegreen D. M., Duc P.-A., Contini T., Epinat B., Shapiro K. L., 2011, ApJ, 730, 4

Bournaud F., Jog C. J., Combes F., 2007, A&A, 476, 1179

Boylan-Kolchin M., Ma C., Quataert E., 2005, MNRAS, 362, 184

Brinchmann J., Ellis R. S., 2000, ApJ, 536, L77

Bruzual G., Charlot S., 2003, MNRAS, 344, 1000

Buitrago F., Trujillo I., Conselice C. J., Bouwens R. J., Dickinson M., Yan H., 2008, ApJ, 687, L61

Buitrago F., Trujillo I., Conselice C. J., Haeussler B., 2011, ArXiv e-prints

Bundy K., Scarlata C., Carollo C. M., Ellis R. S., Drory N., Hopkins P., Salvato M., Leauthaud A., Koekemoer A. M., Murray N., Ilbert O., Oesch P., Ma C.-P., Capak P., Pozzetti L., Scoville N., 2010, ApJ, 719, 1969

Burkert A., Naab T., Johansson P. H., Jesseit R., 2008, ApJ, 685, 897

Caon N., Capaccioli M., D'Onofrio M., 1993, MNRAS, 265, 1013

Cappellari M. e. a., 2012a, ArXiv e-prints

Cappellari M. e. a., 2012b, Nature, 484, 485

Carrasco E. R., Conselice C. J., Trujillo I., 2010, MNRAS, 405, 2253

Cenarro A. J., Trujillo I., 2009, ApJ, 696, L43

Cimatti A., Cassata P., Pozzetti L., Kurk J., Mignoli M., Renzini A., Daddi E., Bolzonella M., Brusa M., Rodighiero G., Dickinson M., Franceschini A., Zamorani G., Berta S., Rosati P., Halliday C., 2008, A&A, 482, 21

Cimatti A., Nipoti C., Cassata P., 2012, MNRAS, 422, L62

Ciotti L., Lanzoni B., Volonteri M., 2007, ApJ, 658, 65

Cole S., Lacey C. G., Baugh C. M., Frenk C. S., 2000, MNRAS, 319, 168

Conroy C., van Dokkum P., 2012, arXiv:1205.6473

Covington M. D., Primack J. R., Porter L. A., Croton D. J., Somerville R. S., Dekel A., 2011, MNRAS, 415, 3135

Cox T. J., Dutta S. N., Di Matteo T., Hernquist L., Hopkins P. F., Robertson B., Springel V., 2006, ApJ, 650, 791

Crocker A. e. a., 2012, MNRAS, 421, 1298

Daddi E., Renzini A., Pirzkal N., Cimatti A., Malhotra S., Stiavelli M., Xu C., Pasquali A., Rhoads J. E., Brusa M., di Serego Alighieri S., Ferguson H. C., Koekemoer A. M., Moustakas L. A., Panagia N., Windhorst R. A., 2005, ApJ, 626, 680

Damjanov I., McCarthy P. J., Abraham R. G., Glazebrook K., Yan H., Mentuch E., LeBorgne D., Savaglio S., Crampton D., Murowinski R., Juneau S., Carlberg R. G., Jørgensen I., Roth K., Chen H.-W., Marzke R. O., 2009, ApJ, 695, 101

De Lucia G., Blaizot J., 2007, MNRAS, 375, 2

De Lucia G., Springel V., White S. D. M., Croton D., Kauffmann G., 2006, MNRAS, 366, 499

de Vaucouleurs G., 1948, Annales d'Astrophysique, 11, 247

Dekel A., Cox T. J., 2006, MNRAS, 370, 1445

Dekel A., Sari R., Ceverino D., 2009, ApJ, 703, 785

Domínguez Sánchez H. e. a., 2011, MNRAS, 417, 900

Dubinski J., 1998, ApJ, 502, 141

Duc P.-A. e. a., 2011, MNRAS, 417, 863

Edwards L. O. V., Patton D. R., 2012, arXiv:1206.1612

Faber S. M. e. a., 2007, ApJ, 665, 265

Farouki R. T., Shapiro S. L., Duncan M. J., 1983, ApJ, 265, 597

Feldmann R., Carollo C. M., Mayer L., 2011, ApJ, 736, 88

Feldmann R., Carollo C. M., Mayer L., Renzini A., Lake G., Quinn T., Stinson G. S., Yepes G., 2010, ApJ, 709, 218

Ferré-Mateu A., Vazdekis A., Trujillo I., Sánchez-Blázquez P., Ricciardelli E., de la Rosa I. G., 2012, MNRAS, 423, 632

Ferreras I., La Barbera F., de Carvalho R. R., de la Rosa I. G., Vazdekis A., Falcon-Barroso J., Ricciardelli E., 2012, arXiv:1206.1594

Franx M., van Dokkum P. G., Schreiber N. M. F., Wuyts S., Labbé I., Toft S., 2008, ApJ, 688, 770

Gabor J. M., Davé R., 2012, ArXiv e-prints

Gerhard O., Kronawitter A., Saglia R. P., Bender R., 2001, AJ, 121, 1936

Governato F., Willman B., Mayer L., Brooks A., Stinson G., Valenzuela O., Wadsley J., Quinn T., 2007, MNRAS, 374, 1479

Graham A. W., Trujillo I., Caon N., 2001, AJ, 122, 1707

Guo Q., White S., Boylan-Kolchin M., De Lucia G., Kauffmann G., Lemson G., Li C., Springel V., Weinmann S., 2011, MNRAS, 413, 101

Guo Q., White S. D. M., 2008, MNRAS, 384, 2

Guo Y., McIntosh D. H., Mo H. J., Katz N., van den Bosch F. C., Weinberg M., Weinmann S. M., Pasquali A., Yang X., 2009, MNRAS, 398, 1129

Hausman M. A., Ostriker J. P., 1978, ApJ, 224, 320

Hernquist L., 1990, ApJ, 356, 359

Hilz M., Naab T., Ostriker J. P., Thomas J., Burkert A., Jesseit R., 2012, arXiv:1206.1597

Hopkins P. F., Bundy K., Hernquist L., Wuyts S., Cox T. J., 2010, MNRAS, 401, 1099

Hopkins P. F., Bundy K., Murray N., Quataert E., Lauer T. R., Ma C.-P., 2009, MNRAS, 398, 898

Hopkins P. F., Cox T. J., Hernquist L., 2008, ApJ, 689, 17

Hopkins P. F., Hernquist L., Cox T. J., Keres D., Wuyts S., 2009, ApJ, 691, 1424

Hoyos C. e. a., 2011, MNRAS, 411, 2439

Hyde J. B., Bernardi M., 2009, MNRAS, 394, 1978

Jiang F., van Dokkum P., Bezanson R., Franx M., 2012, ApJ, 749, L10

Joung M. R., Cen R., Bryan G. L., 2009, ApJ, 692, L1

Kauffmann G., 1996, MNRAS, 281, 487

Kauffmann G., Li C., Fu J., Saintonge A., Catinella B., Tacconi L. J., Kramer C., Genzel R., Moran S., Schiminovich D., 2012, MNRAS, 422, 997

Kereš D., Katz N., Fardal M., Davé R., Weinberg D. H., 2009, MNRAS, 395, 160

Kereš D., Katz N., Weinberg D. H., Davé R., 2005, MNRAS, 363, 2

Khochfar S., Silk J., 2006, ApJ, 648, L21

Kobayashi C., 2004, MNRAS, 347, 740

Kormendy J., Bender R., 2012, ApJS, 198, 2

Kormendy J., Fisher D. B., Cornell M. E., Bender R., 2009, ApJS, 182, 216

Kriek M., van der Wel A., van Dokkum P. G., Franx M., Illingworth G. D., 2008, ApJ, 682, 896

Kriek M., van Dokkum P. G., Franx M., Quadri R., Gawiser E., Herrera D., Illingworth G. D., Labbé I., Lira P., Marchesini D., Rix H.-W., Rudnick G., Taylor E. N., Toft S., Urry C. M., Wuyts S., 2006, ApJ, 649, L71

Kriek M., van Dokkum P. G., Labbé I., Franx M., Illingworth G. D., Marchesini D., Quadri R. F., 2009, ApJ, 700, 221

Lackner C. N., Cen R., Ostriker J. P., Joung M. R., 2012, eprint arXiv:1206.0295

Lackner C. N., Ostriker J. P., 2010, ApJ, 712, 88

Laporte C. F. P., White S. D. M., Naab T., Ruszkowski M., Springel V., 2012, ArXiv e-prints

Longhetti M., Saracco P., Severgnini P., Della Ceca R., Mannucci F., Bender R., Drory N., Feulner G., Hopp U., 2007, MNRAS, 374, 614

López-Sanjuan C., Balcells M., Pérez-González P. G., Barro G., García-Dabó C. E., Gallego J., Zamorano J., 2010, ApJ, 710, 1170

López-Sanjuan C. e. a., 2012, arXiv:1202.4674

Lotz J. M., Jonsson P., Cox T. J., Croton D., Primack J. R., Somerville R. S., Stewart K., 2011, ApJ, 742, 103

Malin D. F., Carter D., 1983, ApJ, 274, 534

Man A. W. S., Toft S., Zirm A. W., Wuyts S., van der Wel A., 2012, ApJ, 744, 85

Mancini C., Daddi E., Renzini A., Salmi F., McCracken H. J., Cimatti A., Onodera M., Salvato M., Koekemoer A. M., Aussel H., Le Floc'h E., Willott C., Capak P., 2010, MNRAS, 401, 933

Mármol-Queraltó E., Trujillo I., Pérez-González P. G., Varela J., Barro G., 2012, MNRAS, 422, 2187

Matteucci F., Francois P., 1989, MNRAS, 239, 885

McIntosh D. H., Guo Y., Hertzberg J., Katz N., Mo H. J., van den Bosch F. C., Yang X., 2008, MNRAS, 388, 1537

McLure R. J., Pearce H. J., Dunlop J. S., Cirasuolo M., Curtis-Lake E., Bruce V. A., Caputi K., Almaini O., Bonfield D. G., Bradshaw E. J., Buitrago F., Chuter R., Foucaud S., Hartley W. G., Jarvis M. J., 2012, ArXiv e-prints

Miller R. H., Smith B. F., 1980, ApJ, 235, 421

Misgeld I., Hilker M., 2011, MNRAS, 414, 3699

Mo H. J., Mao S., White S. D. M., 1998, MNRAS, 295, 319

Moster B. P., Naab T., White S. D. M., 2012, arXiv:1205.5807

Naab T., Burkert A., 2003, ApJ, 597, 893

Naab T., Johansson P. H., Ostriker J. P., 2009, ApJ, 699, L178

Naab T., Johansson P. H., Ostriker J. P., Efstathiou G., 2007, ApJ, 658, 710

Naab T., Khochfar S., Burkert A., 2006, ApJ, 636, L81

Naab T., Ostriker J. P., 2006, MNRAS, 366, 899

Naab T., Ostriker J. P., 2009, ApJ, 690, 1452

Naab T., Trujillo I., 2006, MNRAS, 369, 625

Nelson A. F., Wetzstein M., Naab T., 2009, ApJS, 184, 326

Newman A. B., Ellis R. S., Bundy K., Treu T., 2012, ApJ, 746, 162

Nipoti C., Londrillo P., Ciotti L., 2003, MNRAS, 342, 501

Nipoti C., Treu T., Auger M. W., Bolton A. S., 2009a, ApJ, 706, L86

Nipoti C., Treu T., Bolton A. S., 2009b, ApJ, 703, 1531

Nipoti C., Treu T., Leauthaud A., Bundy K., Newman A. B., Auger M. W., 2012, MNRAS, 422, 1714

Onodera M. e. a., 2012, arXiv:1206.1540

Oser L., Naab T., Ostriker J. P., Johansson P. H., 2012, ApJ, 744, 63

Oser L., Ostriker J. P., Naab T., Johansson P. H., Burkert A., 2010, ApJ, 725, 2312

Ostriker J. P., 1980, Comments on Astrophysics, 8, 177

Ostriker J. P., Hausman M. A., 1977, ApJ, 217, L125

Pipino A., D'Ercole A., Chiappini C., Matteucci F., 2010, MNRAS, 407, 1347

Prantzos N., Aubert O., 1995, A&A, 302, 69

Quilis V., Trujillo I., 2012, ApJ, 752, L19

Ricciardelli E., Trujillo I., Buitrago F., Conselice C. J., 2010, MNRAS, 406, 230

Robaina A. R., Bell E. F., van der Wel A., Somerville R. S., Skelton R. E., McIntosh D. H., Meisenheimer K., Wolf C., 2010, ApJ, 719, 844

Robertson B., Cox T. J., Hernquist L., Franx M., Hopkins P. F., Martini P., Springel V., 2006, ApJ, 641, 21

Ruszkowski M., Springel V., 2009, ApJ, 696, 1094

Saglia R. P. e. a., 2010, A&A, 524, A6

Saracco P., Gargiulo A., Longhetti M., 2012, MNRAS, 422, 3107

Saracco P., Longhetti M., Andreon S., 2009, MNRAS, 392, 718

Schweizer F., Seitzer P., 1992, AJ, 104, 1039

Searle L., Sargent W. L. W., Bagnuolo W. G., 1973, ApJ, 179, 427

Sersic J. L., 1968, Atlas de galaxias australes

Shen S., Mo H. J., White S. D. M., Blanton M. R., Kauffmann G., Voges W., Brinkmann J., Csabai I., 2003, MNRAS, 343, 978

Springel V., 2005, MNRAS, 364, 1105

Szomoru D., Franx M., van Dokkum P. G., 2012, ApJ, 749, 121

Tal T., Wake D. A., van Dokkum P. G., van den Bosch F. C., Schneider D. P., Brinkmann J., Weaver B. A., 2012, ApJ, 746, 138

Taylor E. N., Franx M., Glazebrook K., Brinchmann J., van der Wel A., van Dokkum P. G., 2010, ApJ, 720, 723

Thomas D., Maraston C., Schawinski K., Sarzi M., Silk J., 2010, MNRAS, 404, 1775

Thomas J., Saglia R. P., Bender R., Thomas D., Gebhardt K., Magorrian J., Corsini E. M., Wegner G., 2009, ApJ, 691, 770

Thomas J., Saglia R. P., Bender R., Thomas D., Gebhardt

K., Magorrian J., Corsini E. M., Wegner G., Seitz S., 2011, MNRAS, 415, 545

Tiret O., Salucci P., Bernardi M., Maraston C., Pforr J., 2011, MNRAS, 411, 1435

Toft S., Gallazzi A., Zirm A., Wold M., Zibetti S., Grillo C., Man A., 2012, ArXiv e-prints

Toft S., van Dokkum P., Franx M., Labbe I., Förster Schreiber N. M., Wuyts S., Webb T., Rudnick G., Zirm A., Kriek M., van der Werf P., Blakeslee J. P., Illingworth G., Rix H.-W., Papovich C., Moorwood A., 2007, ApJ, 671, 285

Toft S., van Dokkum P., Franx M., Thompson R. I., Illingworth G. D., Bouwens R. J., Kriek M., 2005, ApJ, 624, L9

Tran K.-V. H., van Dokkum P., Franx M., Illingworth G. D., Kelson D. D., Schreiber N. M. F., 2005, ApJ, 627, L25

Treu T., Ellis R. S., Liao T. X., van Dokkum P. G., 2005, ApJ, 622, L5

Trujillo I., Carrasco E. R., Ferré-Mateu A., 2012, ApJ, 751, 45

Trujillo I., Cenarro A. J., de Lorenzo-Cáceres A., Vazdekis A., de la Rosa I. G., Cava A., 2009, ApJ, 692, L118

Trujillo I., Conselice C. J., Bundy K., Cooper M. C., Eisenhardt P., Ellis R. S., 2007, MNRAS, 382, 109

Trujillo I., Erwin P., Asensio Ramos A., Graham A. W., 2004, AJ, 127, 1917

Trujillo I., Ferreras I., de La Rosa I. G., 2011, MNRAS, 415, 3903

Trujillo I. e. a., 2006, ApJ, 650, 18

Valentinuzzi T., Poggianti B. M., Saglia R. P., Aragón-Salamanca A., Simard L., Sánchez-Blázquez P., D'onofrio M., Cava A., Couch W. J., Fritz J., Moretti A., Vulcani B., 2010, ApJ, 721, L19

van der Wel A., Bell E. F., van den Bosch F. C., Gallazzi A., Rix H., 2009, ApJ, 698, 1232

van der Wel A., Holden B. P., Zirm A. W., Franx M., Rettura A., Illingworth G. D., Ford H. C., 2008, ApJ, 688, 48

van der Wel A., Rix H.-W., Holden B. P., Bell E. F., Robaina A. R., 2009, ApJ, 706, L120

van der Wel A., Rix H.-W., Wuyts S., McGrath E. J., Koekemoer A. M., Bell E. F., Holden B. P., Robaina A. R., McIntosh D. H., 2011, ApJ, 730, 38

van Dokkum P., Conroy C., 2012, arXiv:1205.6471

van Dokkum P. G., 2005, AJ, 130, 2647

van Dokkum P. G., Conroy C., 2010, Nature, 468, 940

van Dokkum P. G., Franx M., Kriek M., Holden B., Illingworth G. D., Magee D., Bouwens R., Marchesini D., Quadri R., Rudnick G., Taylor E. N., Toft S., 2008, ApJ, 677, L5

van Dokkum P. G., Whitaker K. E., Brammer G., Franx M., Kriek M., Labbé I., Marchesini D., Quadri R., Bezanson R., Illingworth G. D., Muzzin A., Rudnick G., Tal T., Wake D., 2010, ApJ, 709, 1018

Villumsen J. V., 1983, MNRAS, 204, 219

Wang J., Kauffmann G., Overzier R., Catinella B., Schiminovich D., Heckman T. M., Moran S. M., Haynes M. P., Giovanelli R., Kong X., 2011, MNRAS, 412, 1081

Weinzirl T., Jogee S., Conselice C. J., Papovich C., Chary R.-R., Bluck A., Grützbauch R., Buitrago F., Mobasher B., Lucas R. A., Dickinson M., Bauer A. E., 2011, ApJ,

743, 87

Wetzstein M., Nelson A. F., Naab T., Burkert A., 2009, ApJS, 184, 298

Whitaker K. E., Kriek M., van Dokkum P. G., Bezanson R., Brammer G., Franx M., Labbé I., 2012, ApJ, 745, 179

Whitaker K. E., van Dokkum P. G., 2008, ApJ, 676, L105

White S. D. M., 1978, MNRAS, 184, 185

White S. D. M., 1979, MNRAS, 189, 831

Williams R. J., Quadri R. F., Franx M., 2011, ApJ, 738, L25

Williams R. J., Quadri R. F., Franx M., van Dokkum P., Toft S., Kriek M., Labbé I., 2010, ApJ, 713, 738

Wuyts S., Cox T. J., Hayward C. C., Franx M., Hernquist L., Hopkins P. F., Jonsson P., van Dokkum P. G., 2010, ApJ, 722, 1666

Wuyts S. e. a., 2011, ApJ, 742, 96

Yang X., Mo H. J., van den Bosch F. C., Zhang Y., Han J., 2011, ArXiv e-prints

Yang X., Mo H. J., van den Bosch F. C., Zhang Y., Han J., 2012, ApJ, 752, 41

Young L. M. e. a., 2011, MNRAS, 414, 940

Zirm A. W., van der Wel A., Franx M., Labbé I., Trujillo I., van Dokkum P., Toft S., Daddi E., Rudnick G., Rix H., Röttgering H. J. A., van der Werf P., 2007, ApJ, 656, 66